Mechanical Systems and Signal Processing 62-63 (2015) 431–443

Contents lists available at ScienceDirect

Mechanical Systems and Signal Processing

journal homepage: www.elsevier.com/locate/ymssp

A novel quality evaluation method for resistance spot welding based on the electrode displacement signal and the Chernoff faces technique

Hongjie Zhang [a,*], Fujun Wang [b], Tao Xi [a], Jian Zhao [c], Lijing Wang [c], Weiguo Gao [b]

[a] Tianjin Key Laboratory of Modern Mechatronics Equipment Technology, School of Mechanical Engineering, Tianjin Polytechnic University, Tianjin 300387, China
[b] Tianjin Key Laboratory of Equipment Design and Manufacturing Technology, School of Mechanical Engineering, Tianjin University, Tianjin 300072, China
[c] School of Control and Mechanical, Tianjin Chengjian University, Tianjin 300384, China

ARTICLE INFO

Article history:
Received 1 September 2014
Received in revised form
3 March 2015
Accepted 5 March 2015
Available online 26 March 2015

Keywords:
Resistance spot welding
Quality evaluation
Signal processing
Chernoff faces
Feature extraction
Data visualizations

ABSTRACT

To develop a visual and reliable weld quality assessment method for resistant spot welding, the electrode displacement signal was measured and analyzed. Some statistical features closely related to the weld quality were extracted. The multi-dimensional extracted features from the signal were sketched as Chernoff face which characterizes the welding quality through the different facial expressions. The weld quality was summarized as four levels, namely poor, good, excellent and expulsion, and each level corresponded to one kind of facial expression. By visual judgment, good or bad welds were identified accurately and rapidly even though the weld was made under abnormal welding conditions. In particular, the visual characteristic makes the diagnostic procedure for welding quality easily understood and interpreted.

1. Introduction

Owing to high efficiency, suitability and low cost, resistance spot welding (RSW) plays an important role in the automotive industry [1]. However, the RSW suffers from a serious inconsistent quality problem. Conventional destructive test methods, such as tension shear, cross-tension shear, twist and peel tests, can ensure the qualities of some specific welds, while they bring product wastage and labor costs. Consequently, non-destructive test methods based on the dynamic signals during RSW process have recently received considerable attentions [2–4]. Various dynamic signals had been measured and different kinds of signal processing technologies were proposed to monitor or control the welding and joining quality [5,6]. The electrode displacement signal during the RSW process is mainly caused by the thermal expansion of the weld nugget, and it can make fast response to small changes of any variables affecting the welding quality [7,8]. It is believed that the amount of the thermal expansion, melting, expulsion, electrode wear and the mechanical features of the welding machine

* Corresponding author. Tel.: +86 2283955131; fax: +86 2283955258.
E-mail address: zhanghj022@163.com (H. Zhang).

http://dx.doi.org/10.1016/j.ymssp.2015.03.007
0888-3270/

can be revealed by the magnitude, slope and fluctuation of the displacement curve [9–12]. Lots of measurement methods were used in order to acquire the electrode displacement signal [13–17].

At present, weld quality assessment based on the dynamic signals can be classified as quality prediction and classification. For quality prediction, the multiple regression analysis and the artificial neural network-based methods are widely used to establish the correlation between the monitored features and quality indicators. Hao et al. [18] and Cho et al. [19] used the multiple linear regression analysis to predict weld size and strength. Luo et al. [20] selected nonlinear regression analysis to develop the mapping model between the welding parameters and the quality indicators. Cho et al. [21] predicted the tensile-shear strength of the weld based on the back-propagation neural network. By using the radial basis function neural network, Zhang et al. [22] revealed the correlation between the weld strength and the monitored features extracted from the electrode displacement signal. To achieve good welding, Hamidinejad et al. [23] combined genetic algorithm with neural network to optimize welding parameters. Zhang et al. [24] proposed a nondestructive quality estimation method on the basis of the principal component analysis and the support vector machine technique.

To realize quality classification, the weld quality is usually classified into several categories, and then the data mining and neural network-based methods are widely adopted to develop classifier. Zhao et al. [25] used the linear vector quantization neural network to classify the welding quality. Podržaj et al. [26] selected the same neural network to monitor the expulsion phenomenon during the RSW process. Zhang et al. [27] constructed a weld quality classifier by using an associative memory network. Martín et al. [28] got the weld quality information based on multilayer feed-forward network. Ling et al. [29] regarded the electrical input impedance of the welding machine as the monitored signal and designed a classifier to evaluate the welding quality. Zhang et al. [30] adopted the probabilistic neural network to distinguish good or bad welds.

When using the artificial intelligence technology or machine learning method to evaluate the welding quality, the assessment process is usually invisible, just like a “black box” resulting in the difficulties in understanding and interpreting the evaluation procedure. The aim of this paper is to develop a visual and reliable quality evaluation method, in which the electrode displacement signal during the RSW process is measured and analyzed. Some features extracted from the displacement curve are regarded as facial variables to draw a Chernoff face, and then a novel and interesting method for welding quality classification is discussed. Good welding is always enjoyable and bad one is always disappointing. Through observing the facial expression on the Chernoff face, the welding quality can be understood rapidly, accurately and vividly.

1.1. Experimental setup and the electrode displacement signal

The measurement system for the electrode displacement signal is schematically shown in Fig. 1, and it was composed of an AC resistance spot welding machine, sensors, signal acquisition device and computer. When the welding current flows through the workpieces, a volume of material at the faying surfaces between workpieces melts and forms the nugget due to the joule heating. A linear variable differential transformer displacement sensor with a resolution of 0.01 μm was used to measure the movement of the upper electrode. The welding current signal was measured synchronously using a commercial Rogowsky coil, and it was used to calculate the effective value of the welding current. These two signals were input into a data acquisition device NI USB6366 whose sample rate was set as 400 kHz.

The lapping welding was performed on a 0.7-mm-thick sheet of uncoated low-carbon steel and the work pieces were cut as 120×30 mm^2. The face diameter of cone electrode was 6 mm. The welding time and force were set as 400 ms and 2.0 kN, respectively. When the welding current was increased with 0.2 kA intervals starting from 3.2 to 4.4 kA, a number of weld specimens were obtained. A typical electrode displacement waveform from 4.4 kA welding current is shown in Fig. 2(a), where the acquisition time for the signal was 500 ms. In order to remove the high-frequency noise in the signal, the wavelet de-noising method was adopted and the result is displayed in Fig. 2(b). As shown, the electrode displacement curve experiences three phases named rising phase, stable phase and dropping phase, respectively. At the beginning of the rising

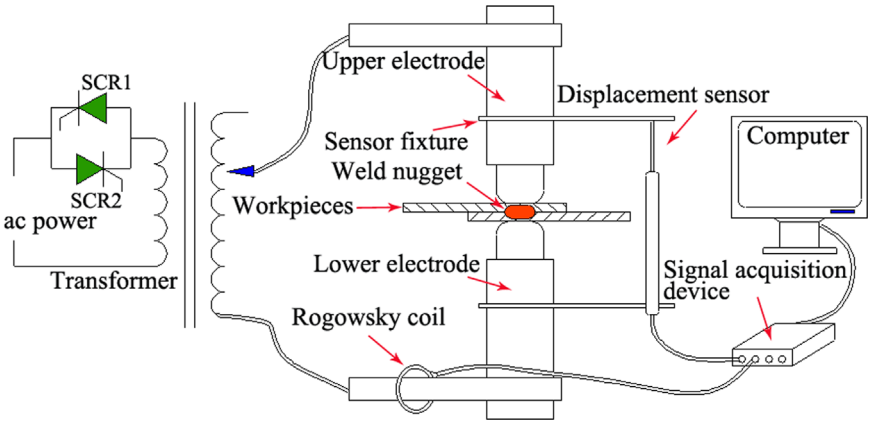

Fig. 1. The schematic diagram of the experimental setup.

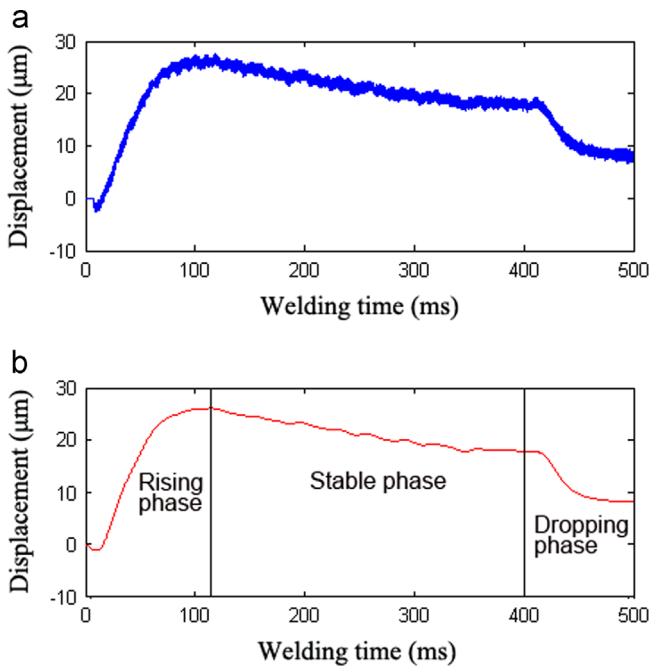

Fig. 2. (a) A typical electrode displacement signal, and (b) the displacement signal through noise reduction.

phase, the displacement curve tends to drop because the electrode force brings the workpieces into contact. With the accumulation of joule heat, the nugget births and grows. The volume change from the solid to liquid causes the displacement curve to rise to its peak rapidly. When the nugget size exceeds the electrode tip diameter and reaches saturation, the displacement curve enters to a relatively stable phase, where a slow descent can be observed. This phenomenon can be attributed to the softening of the material and a gradual increase in weld indentation depth. In the dropping phase, the welding current is cut off and the curve drops rapidly.

As known, the weld nugget size is well correlated with the weld strength and it generally increases with the increasing welding current if other welding parameters remain constant, that is, higher welding current brings greater thermal expansion, better weld size and strength. Lower welding current results in poorer weld size even no weld. To observe the change rules of the displacement curves with different welding currents, 10 displacement curves under each current parameter were recorded. For each displacement curve, a series of half-cycle (10 ms) average values were calculated. Thus, the data quantity of one displacement curve could be reduced to 50. Then, we got the mean curve of these 10 displacement curves from the same welding current. Fig. 3 provides the curved surface constructed by these mean curves. These mean curves do experience similar change process, differing only in amplitude, time lengths of the rising phase and the stable phase.

During the RSW process, the weld nugget does not always reach its optimal size when using appropriate welding parameters. Actually, the nugget will collapse as the solid material around the nugget is no longer able to withstand the pressure of the electrodes. The result is an expulsion of the molten material at the faying surface or the electrode workpiece interface. Expulsion should be avoided because it destroys the energy absorption capability of the weld as well as the corrosion resistance of the coated materials. Moreover, it brings unsatisfactory visual appearance, high electrode wear and energy consumption [31,32]. Compared with the electrode displacement curve from the normal welding, a sudden drop is seen when the expulsion occurs, as shown in Fig. 4.

2. Feature extraction for the electrode displacement signal

To develop an effective method to evaluate the welding quality, feature extraction and selection for the electrode displacement signal are necessary. In this research, nine time domain statistical characteristics were extracted and five of them are schematically indicated in Fig. 5. Point *a* in this figure is the peak time corresponding to the displacement amplitude maximum. Points *b* and *c* correspond to the welding stop time and signal stop time, respectively. The detailed descriptions and equations for extracted features are provided in Table 1, where $d(t)$ represents the measured displacement amplitude series. n is the amount of sampling data which can be obtained from the product of welding time and sample rate.

For each welding current, 10 weld samples were selected, in addition, 10 welds from expulsion welding were considered as well, thus, a total of 80 weld specimens composed a sample set. When the feature extraction was finished, a multivariate data set was obtained. The scatter diagrams for nine extracted features are shown in Fig. 6. Considering that there are great

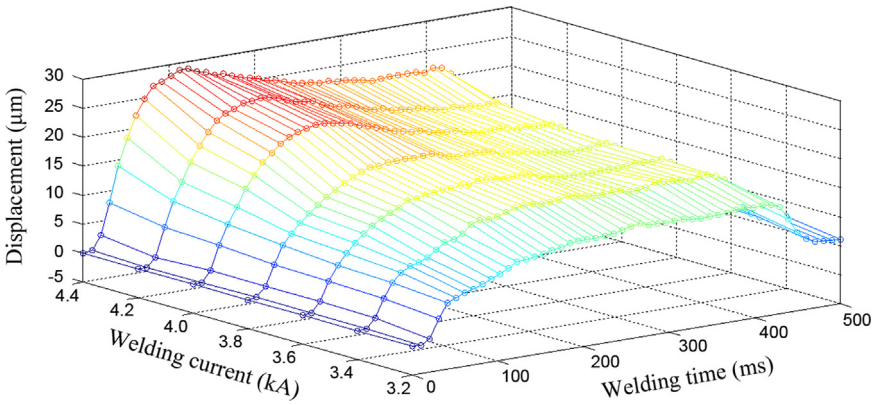

Fig. 3. Curved surface of the electrode displacement curves.

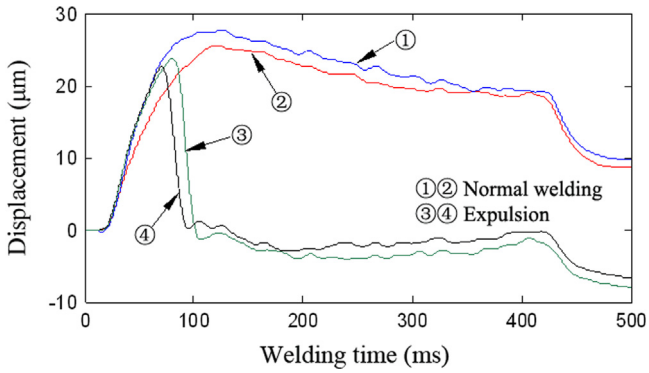

Fig. 4. Comparisons of the displacement curves between normal welding and expulsion.

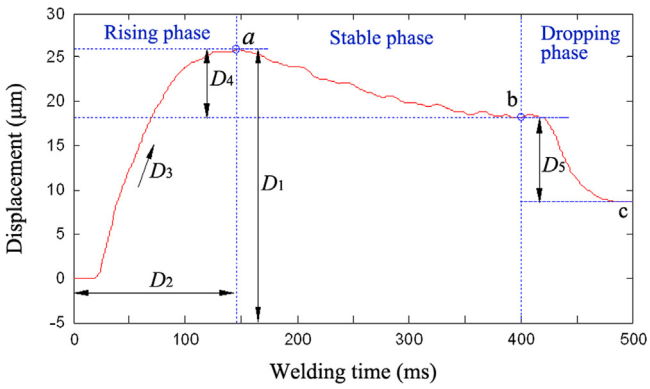

Fig. 5. The schematic diagram for some extracted features of the displacement curve.

differences among the numeric values of some features, the scatter diagrams for these features from the expulsion welds are provided separately, as shown in Fig. 6(d),(f) and (i).

3. Chernoff faces method

Data visualizations describe the multi-dimensional data in a graphical format providing human with a quick qualitative understanding. These technologies play an important role in a wide range of applied areas, such as intelligence analysis, information retrieval and data mining. Chernoff face is an interesting method to describe the multi-dimensional data through facial characteristics and expressions. The facial characteristics on a typical human face consist of face, eyes, pupils, eyebrows, nose and mouth [33,34]. In this research, 17 facial attributes shown in Fig. 7 were utilized to draw the face and

Table 1
Descriptions and equations for the features extracted from the electrode displacement signal.

Features	Description	Equation
D_1	The maximum electrode displacement.	$D_1 = \max(d(t)),\ \ t = 1, 2, 3, \cdots, n$
D_2	The rising phase time	$D_2 = a$
D_3	The rising phase rate	$D_3 = D_1/D_2$
D_4	The displacement amplitude decrease in the stable phase	$D_4 = d(a) - d(\mathrm{b})$
D_5	The displacement amplitude decrease in dropping phase	$D_5 = d(\mathrm{b}) - d(\mathrm{c})$
D_6	The mean value of the displacement amplitude during welding process	$D_6 = \frac{1}{n}\sum_{t=1}^{n} d(t)$
D_7	The root mean square value of the displacement amplitude during welding process	$D_7 = \sqrt{\frac{1}{n}\sum_{t=1}^{n} d(t)^2}$
D_8	The variance value of the electrode displacement amplitude during welding process	$D_8 = \frac{1}{n}\sum_{t=1}^{n} (d(t) - D_6)^2$
D_9	The skewness value the electrode displacement amplitude during welding process	$D_9 = (\frac{1}{n}\sum_{t=1}^{n} (d(t) - D_6)^3)/{D_8}^{3/2}$

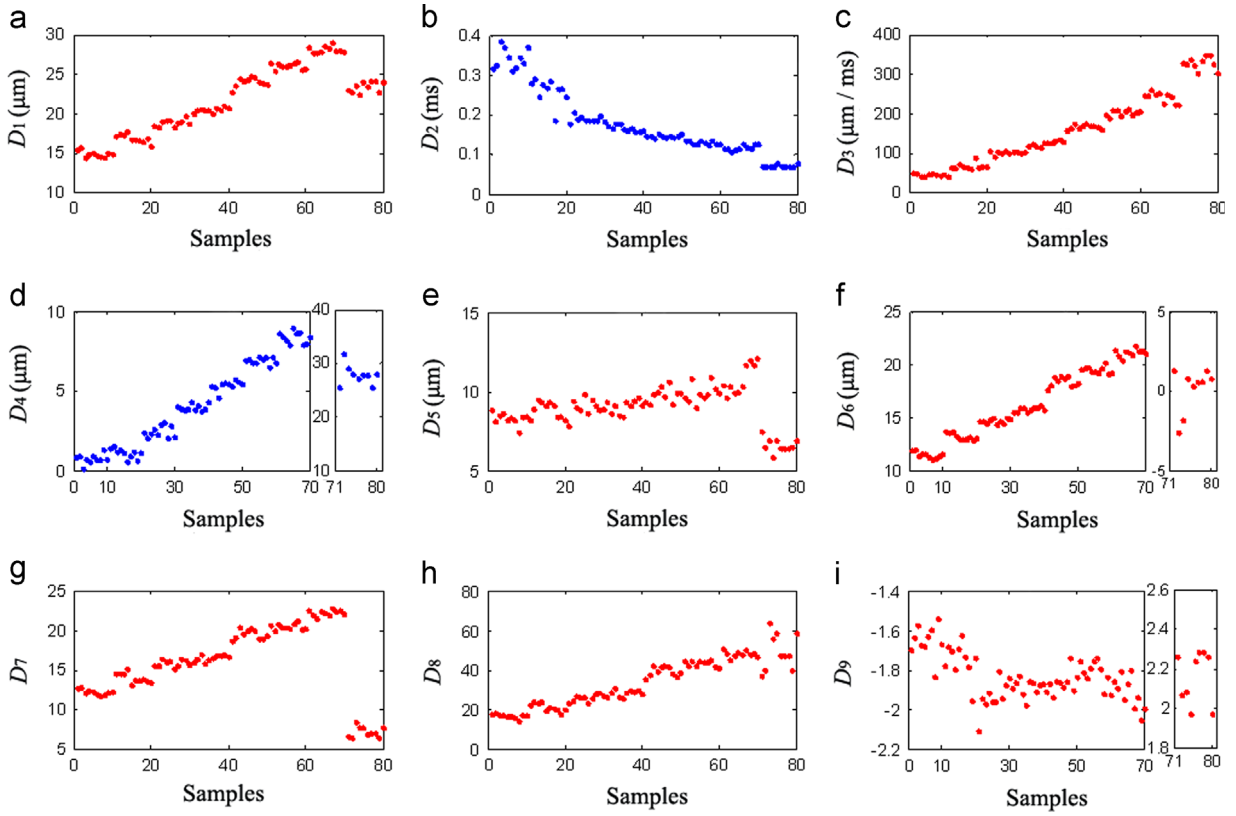

Fig. 6. The scatter diagrams of the extracted features.

a brief description for each attribute is provided in Table 2. To obtain the analytic equations that these facial attributes need to satisfy, 17 facial variables (X_1–X_{17}) were considered, then the following work has been done:

(1) The outline of the face.
As shown in Fig. 7, the outline of the face consists of upper and lower ellipses. These two ellipses respectively represent forehead and jaw, and they intersect at points A and A′. The distance between A and the origin O is defined by the attributes F_r and F_a.

$$F_r = 0.5 + 1.5X_1 \tag{1}$$

$$F_a = 0.7\pi(X_2 - 0.5) \tag{2}$$

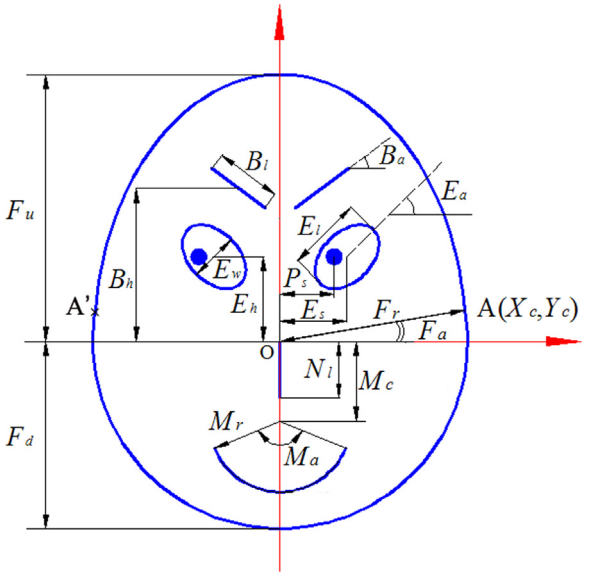

Fig. 7. The Chernoff face and its attributes.

Table 2
Descriptions of the facial attributes.

Facial feature	Description
F_r	Face size
F_a	Relative arc length of the forehead or jaw
F_u	Forehead shape
F_d	Jaw shape
E_s	Width between eyes
E_h	Vertical position of the eyes
E_l	Height of the eyes
E_w	Width of the eyes
E_a	Angle of the eyes
B_h	Vertical position of the eyebrows
B_l	Width of the eyebrows
B_a	Angle of the eyebrows
P_s	Direction of the pupils
N_l	Nose length
M_c	Vertical position of the mouth
M_r	Radius of the arc for the mouth
M_a	Central angle of the arc for the mouth

thus

$$X_c = F_r \cos(F_a) \tag{3}$$

$$Y_c = F_r \sin(F_a) \tag{4}$$

Based on the knowledge of the analytic geometry, the trajectory equation for the upper ellipse can be expressed as

$$\frac{x^2}{a_u^2}+\frac{y^2}{F_u^2}=1 \tag{5}$$

where a_u is the horizontal axis of the upper ellipse. Similarly, the trajectory equation of the lower ellipse is

$$\frac{x^2}{a_d^2}+\frac{y^2}{F_d^2}=1 \tag{6}$$

where a_d is the horizontal axis of the lower ellipse.
For the upper and lower ellipses, if the length ratios between the vertical and horizontal axes are defined as

$$T_u = F_u/a_u = 0.5(1+3X_3) \tag{7}$$

$$T_d = F_d/a_d = 0.5(1+3X_4) \tag{8}$$

the trajectory equations of the forehead and jaw ellipses can be deduced accordingly

$$\frac{x^2}{a_u^2}+\frac{y^2}{T_u^2 a_u^2}=1 \tag{9}$$

$$\frac{x^2}{a_d^2}+\frac{y^2}{T_d^2 a_d^2}=1 \tag{10}$$

where

$$a_u = \sqrt{X_c^2+(Y_c/T_u)^2} \tag{11}$$

$$a_d = \sqrt{X_c^2+(Y_c/T_d)^2} \tag{12}$$

(2) The outlines of the eye and pupil.
Two eyes in the face are also depicted as two ellipses and some important attributes are defined as follows:

$$E_s = 0.25(1+2X_5)X_c \tag{13}$$

$$E_h = 0.35X_6(F_u-F_d)+0.5(F_u+F_d) \tag{14}$$

$$E_w = 0.5X_8+0.55 \tag{15}$$

$$E_l = 0.3X_7+0.075 \tag{16}$$

$$E_a = 0.3\pi(X_9-0.5) \tag{17}$$

We often express our feelings through eye movements, therefore, the rotating feature of the ellipse is concerned. The rotation equation of the ellipse can be written as

$$\frac{x'^2}{E_w^2}+\frac{y'^2}{E_l^2}=1 \tag{18}$$

where

$$x' = x\ \cos(E_a)-y\ \sin(E_a)+E_s \tag{19}$$

$$y' = x\ \sin(E_a)+y\ \cos(E_a)+E_h \tag{20}$$

Eye gaze is an important component of the facial information, in this research, the location of the pupil is decided by the attributes P_h and P_s. The height of the pupil P_h is equal to E_h , and the direction of the pupil P_s is decided by

$$P_s = E_s+1.5E_l(X_{13}-0.5) \tag{21}$$

(3) The outlines of the eyebrow and nose.
The eyebrow and nose are simply sketched as lines. Some attributes of the eyebrow are listed as follows:

$$B_h = 0.5F_uX_{10}+(1-0.5X_{10})E_hE_w \tag{22}$$

$$B_l = 0.3X_{11}+0.075 \tag{23}$$

$$B_a = 0.1\pi(X_{12}-0.5) \tag{24}$$

Eq. (25) provides the linear equation for the eyebrow

$$y = \tan(B_a+E_a)(x+E_s)+B_h \tag{25}$$

The length of the nose line is decided by

$$N_l = 0.7X_{14}(E_h-F_d) \tag{26}$$

(4) The outline of the mouth.
The mouth plays an important role to express emotion and it is drawn with an arc whose length is determined by the

central angle and the circle radius. The circle equation for the mouth is

$$\frac{x^2}{M_r^2}+\frac{(y-M_c)^2}{M_r^2}=1 \tag{27}$$

where M_c is the ordinate value of the central coordinate. M_r and M_a are the radius and central angle of the circle, respectively. M_c, M_r and M_a are decided by

$$M_c=(E_h-N_l)X_{15}+F_d(1-X_{15})+M_r \tag{28}$$

$$M_r=6X_{16}-2.7 \tag{29}$$

$$M_a=0.5\pi X_{17} \tag{30}$$

If some features extracted from the electrode displacement curve are viewed as facial variables, a Chernoff face can be drawn. It is expected to provide a novel approach for welding quality assessment.

4. Welding quality evaluation for RSW

The tensile-shear strength of the weld was examined as the welding quality indicator. Fig. 8 shows the measured strengths of the weld specimens in the sample set previously mentioned. The strength criterion of 2.89 kN, which determines good and poor welds, is plotted as a dot line. It can be observed that if a weld is made using a smaller welding current than 3.8 kA, it will present poor quality. With the welding current increasing to 3.8 kA, the weld strength is obviously higher than the strength criterion and it is considered as good welding. As the welding current increases further, the weld strength increases further as well. If the strength exceeds 3.3 kN, the weld will be viewed as an excellent welding. Because the expulsion is considered undesirable, the strengths of the expulsion welds are not provided in Fig. 8. So far the weld quality can be summarized as four levels, namely poor, good, excellent and expulsion.

Feature selection is an important process in drawing the Chernoff faces. Generally, two methods can be used for feature selection: one is correlation analysis and the another is principal component analysis [35]. In this study, the correlation analysis was carried out and the correlation coefficients between the extracted features and the weld strengths are listed in Table 3. Only feature D_9 has relatively low correlation with weld strength. Seven features with relatively high correlation coefficients are regarded as facial variables to sketch the Chernoff face and the substitution results are listed in Table 3.

As previously mentioned, drawing Chernoff face needs 17 facial variables, therefore, the facial variables unsubstituted by the selected features are initialized with default value of 0.5. Through normalizing all facial variables into the range of 0.05–0.9, the Chernoff faces corresponding to weld specimens can be drawn. For each welding current parameter, five Chernoff faces were selected and shown in Fig. 9. As the authors expect that the faces carry rich facial information. With the increase of weld strength, the facial expression changes significantly. For poor welding, disappointment is etched on the face. For good welding, the face takes on an expression of cool. When the weld quality is excellent, the face is filled with smile, nevertheless, for

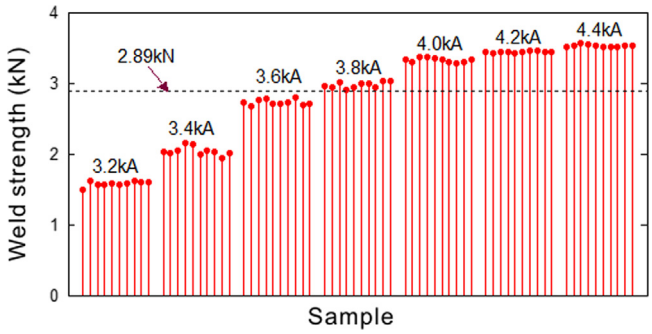

Fig. 8. The tensile-shear strengths of the weld specimens.

Table 3
Results of the correlation analysis and the feature selection.

Monitored features	D_1	D_2	D_3	D_4	D_5	D_6	D_7	D_8	D_9
Correlation coefficient	0.9399	−0.9698	0.9298	0.9212	0.9013	0.9488	0.9489	0.9002	−0.6294
Facial variables	X_{13}	X_{12}	X_{11}	X_{17}	X_9	X_5	X_{16}	–	–

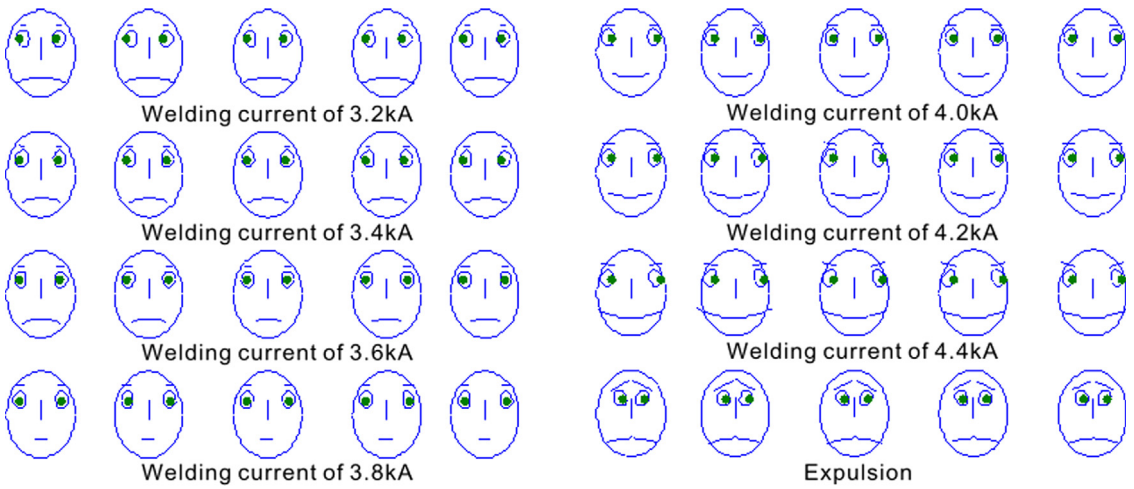

Fig. 9. The constructed Chernoff faces.

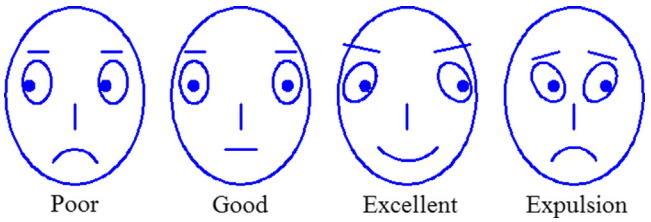

Fig. 10. Chernoff face templates corresponding to different weld quality levels.

expulsion it shows another picture, sorrow and grievance are expressive. Thus, the Chernoff faces can also be summarized as four templates shown in Fig. 10. Each template opportunely corresponds to one kind of welding quality level. As a consequence, a novel and interesting welding quality assessment method has been developed. If the Chernoff face of a certain weld matches up with one kind of template, the weld quality can be understood.

In order to examine the performance of the Chernoff faces method, 90 test weld samples were selected. The tensile-shear strengths of these welds are provided in Fig. 11(a), where the strength criterion is expressed as a plane. The strengths of the expulsion welds (such as welds 4, 8, 21 and 22) are not shown. The test results are shown in Fig. 11(b) and all test samples can be classified correctly. Thirty test samples marked in Fig. 11 were chosen to show their Chernoff faces (see Fig. 12). From the test results, it can be confirmed that the Chernoff face can help us judge the weld quality well.

5. Quality evaluation for abnormal welding

In industrial applications of RSW, the welding quality is significantly influenced by various disturbances, such as shunting, small edge distance, greasy surface and so on. It is important for a reliable quality assessment method to correctly judge the quality of the weld from the abnormal welding process. To test the validation of the proposed method for the abnormal welds, shunting and small edge distance welding were considered.

Shunting in RSW is the diversion of the welding current from the weld to be made (named shunted weld) to a nearby existing weld (named shunt weld). The electrode displacement curves from normal welding and shunting, together with their corresponding Chernoff faces, are compared in Fig. 13(a), where three curves are all from 4.4 kA welding current and curves (1), (2) and (3) respectively correspond to normal, two-, and four-weld shunting welding. The schematic diagrams for the designed shunting welding specimens are shown in Fig. 13(b). Before making the shunted weld (marked in Fig. 13(b)), two or four premade neighboring shunt welds already exist. Thus, shunting will occur during the spot welding process of the shunted weld. As the applied electric current is shared by the shunted weld and some shunt welds, the heat generation in shunted weld is not sufficient for it to grow to the expected size. As a consequence, the slop and amplitude of the curves from shunting welding change more obviously compared with curve (1) from normal welding. These differences can also be reflected by the facial expressions on their corresponding Chernoff faces.

When the workpieces are welded with a small edge distance, the area for heat dissipation decreases. So the temperature in the welding region increases rapidly at the early stage of the welding process. However, due to the small constraint caused by the surrounding cold material adjacent to the workpiece edge, the expansion of the nugget is much easier in the

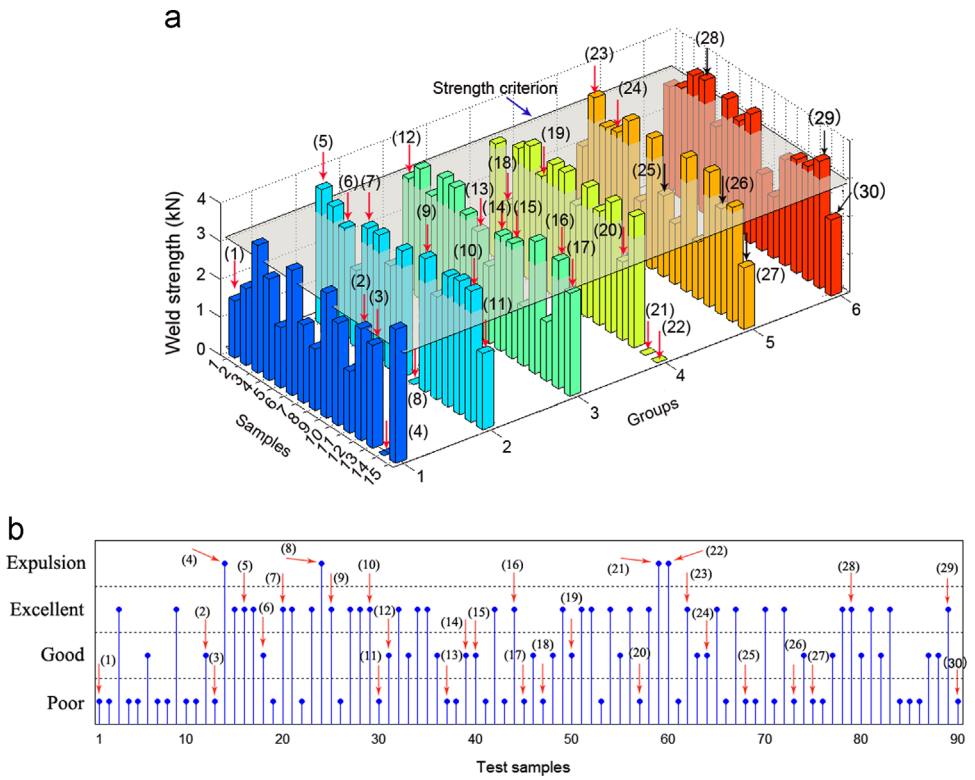

Fig. 11. (a) Measured tensile-shear strengths of the test weld samples, and (b) weld quality classification results.

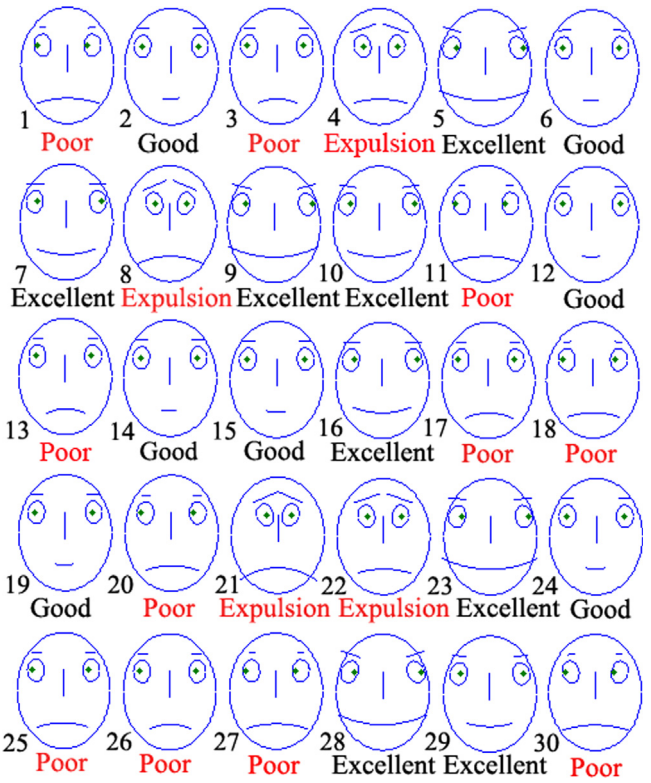

Fig. 12. Chernoff faces of some test welds.

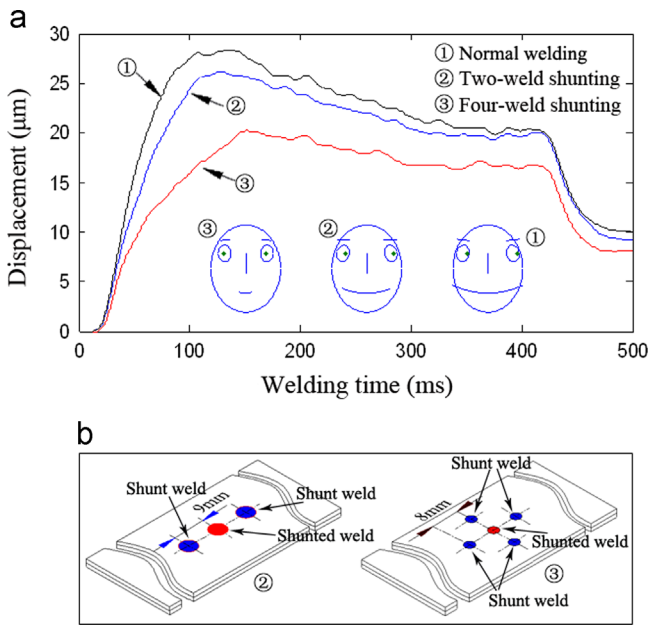

Fig. 13. (a) Comparisons of the electrode displacement curves and their corresponding Chernoff faces between normal and shunting welding, and (b) the schematic diagram of the designed weld specimens for two-, four-weld shunting.

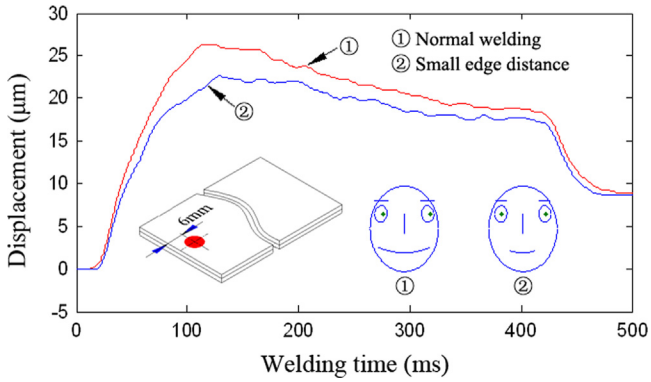

Fig. 14. Comparisons of the electrode displacement curves and their corresponding Chernoff faces between normal and small edge distance welding.

weld nugget growing period. Thus, the displacement amplitude curve from small edge distance welding is less than the normal one, as shown in Fig. 14. It also can be embodied by distinct expression changes on the Chernoff faces.

Thirty-two weld specimens from abnormal welding processes were used to test the performance of the Chernoff faces method. The test results are shown in Fig. 15, where the applied welding current for each weld is shown as well. All welds can be properly classified. Eight test welds marked in Fig. 15 were selected to show their Chernoff faces in Fig. 16. For instance, the Chernoff face of the test weld 1, which was from small edge distance welding, shows an expression of poor welding despite this weld was welded using 3.8 kA welding current. A similar case happens to the test weld 6 (with the welding current of 4.0 kA) from two-weld shunting welding. An interesting phenomenon is observed from the classification results of test welds 2 and 3 made under small edge distance welding condition. When these two test welds were made using 4.4 kA welding current, expulsion occurred early in their respective spot welding processes. It means that expulsion tends to happen when small edge distance welding is done using higher welding currents. Fortunately, this situation can be reflected well by the facial expression on Chernoff face.

6. Conclusions

This research proposes a novel and interesting approach to assess the welding quality. The multi-dimensional features extracted from the electrode displacement signal during the RSW process were viewed as the facial variables to draw the

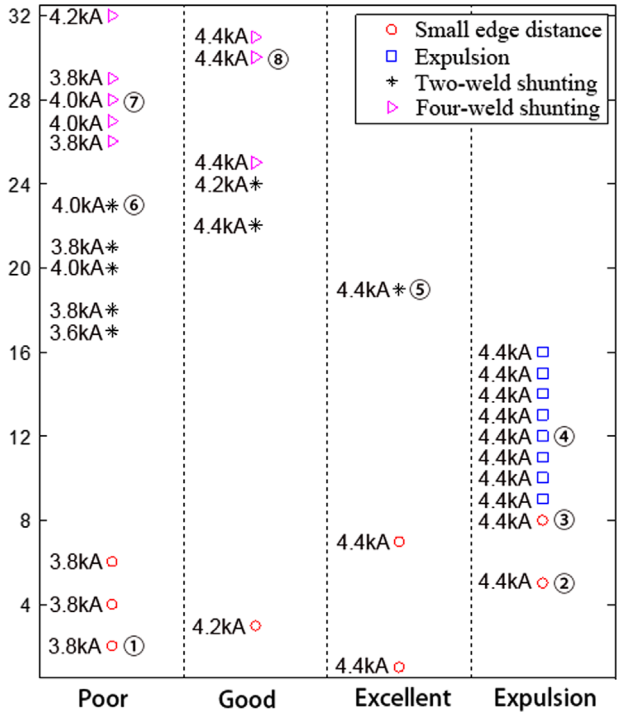

Fig. 15. Classification results of the test welds from abnormal welding processes.

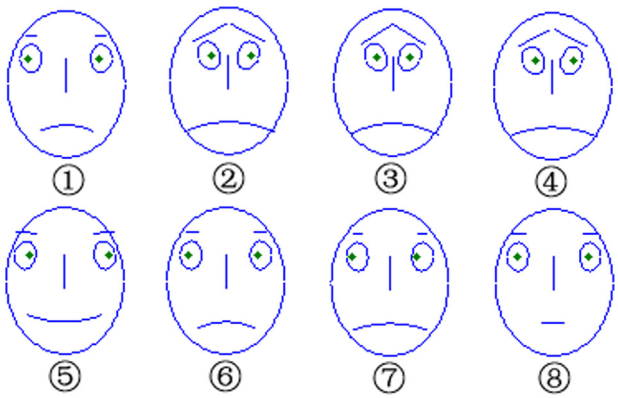

Fig. 16. Chernoff faces of some selected test welds from abnormal welding.

Chernoff faces. Through observing the facial expression, the quality information of the weld can be understood. Following results have been obtained:

1. Compared with the complex algorithms for revealing the correlation between the monitored features and quality indicators, the Chernoff faces method is faster, more simple and efficient. It is feasible and reliable to describe the multi-dimensional features extracted from the electrode displacement signal as Chernoff face.
2. Chernoff faces can reflect the welding quality levels through different facial expressions. Human can obtain the weld quality information accurately and rapidly even though the weld is from abnormal welding process, in particular, the visual characteristic makes the diagnostic procedure for welding quality understood and interpreted easily.
3. Undeniable, drawing the faces primarily depends on human's subjective judgments and it requires some work to select the reasonable variables and methods to draw the ideal face. Anyway, it is a new attempt for welding quality evaluation based on signal processing technologies. Meanwhile, the method contains much useful and practical information for the manufacturing processes using the resistance spot welding or other welding and joining techniques.
4. If the facial expression on the Chernoff face can be distinguished by computer, the welding quality assessment results will be more accurate, and it also can put human out of the control loop. This will be further studied. In addition, only

mild steel material is considered to investigate the performance of proposed method in this research, the performance for some modern steels will be further studied.

Acknowledgments

This work is supported by the National Natural Science Foundation of China (Grant no. 51205279 and 51275337), the Natural Science Fund of Tianjin (Grant no. 11JCYBJC06200), the Science & Technology Commission of Tianjin Municipality (Grant no. 13JCQNJC04100), and the Tianjin University for Peiyang Elite Scholar (Grant no. 60301014). The authors would like to express their gratitude.

References

[1] M. Ouisse, S. Cogan, Robust design of spot welds in automotive structures: a decision- making methodology, Mech. Syst. Signal Process. 24 (2010) 1172–1190.
[2] P. Podržaj, I. Polajnar, J. Diaci, Z. Kariž, Overview of resistance spot welding control, Sci. Technol. Weld. Join. 13 (2008) 215–224.
[3] C.S. Chien Jr., Kannatey Asibu, Investigation of monitoring systems for resistance spot welding, Weld. J. 81 (2002) 195s–199s.
[4] P. Podržaj, S. Simončič, Resistance spot welding control based on the temperature measurement, Sci. Technol. Weld. Join. 18 (2013) 551–557.
[5] W.W. Feng, Q.F. Meng, Y.B. Xie, H. Fan, Wire bonding quality monitoring via refining process of electrical signal from ultrasonic generator, Mech. Syst. Signal Process. 25 (2011) 884–900.
[6] D.Y. You, X.D. Gao, S.J. Katayama, Monitoring of high-power laser welding using high-speed photographing and image processing, Mech. Syst. Signal Process. 49 (2014) 39–52.
[7] D.F. Farson, J.K. Chen, K. Ely, T. Frech, Monitoring resistance spot nugget size by electrode displacement, J. Manuf. Sci. Eng. 126 (2004) 391–394.
[8] S.A. Gedeon, C.D. Sorenson, K.T. Ulrich, T.W. Eagar, Measurement of dynamic electrical and mechanical properties of resistance spot welds, Weld. J. 66 (1987) 378s–385s.
[9] S. Simončič, P. Podržaj, Resistance spot weld strength estimation based on electrode tip displacement velocity curve obtained by image processing, Sci. Technol. Weld. Join. 19 (2014) 468–475.
[10] C.L. Tsai, W.L. Dai, D.W. Diskinson, Analysis and development of a real-time control methodology in resistance spot welding, Weld. J. 70 (1991) 339s–351s.
[11] H. Tang, W. Hou, S.J. Hu, Influence of welding machine mechanical characteristics on resistance spot welding process and weld quality, Weld. J. 85 (2003) 116–124.
[12] M. Jou, Real time monitoring weld quality of resistance spot welding for the fabrication of sheet metal assemblies, J. Mater. Process. Technol. 132 (2003) 102–113.
[13] Y.S. Zhang, H. Wang, G.L. Chen, Monitoring and intelligent control of electrode wear based on a measured electrode displacement curve in resistance spot welding, Meas. Sci. Technol. 18 (2007) 867–876.
[14] J.Z. Chen, D.F. Farson, Electrode displacement measurement dynamics in monitoring of small scale resistance spot welding, Meas. Sci. Technol. 15 (2004) 2419–2425.
[15] C.T. Ji, Y. Zhou, Dynamic electrode force and displacement in resistance spot welding of aluminum, ASME: J. Manuf. Sci. Eng. Trans. 126 (2004) 606–610.
[16] L. Kučšer, I. Polajnar, J. Diaci., A method for measuring displacement and deformation of electrode during resistance spot welding, Meas. Sci. Technol. 15 (2011) 592–598.
[17] S. Simončič, P. Podržaj, Image-based electrode tip displacement in resistance spot welding, Meas. Sci. Technol. 23 (2012) 1–7.
[18] M. Hao, K.A. Osman, Development in characterization of the resistance spot welding of aluminum, Weld. J. 75 (1996) 1s-8s.
[19] Y. Cho, S. Rhee, Primary circuit dynamic resistance monitoring and its application to quality estimation during resistance spot welding, Weld. J. 81 (2002) 104s–111s.
[20] Y. Luo, J.H. Liu, H.B. Xu, C.Z. Xiong, L. Liu, Regression modeling and process analysis of resistance spot welding on galvanized steel sheet, Mater. Des. 30 (2009) 2547–2555.
[21] Y. Cho, S. Rhee, New technology for measuring dynamic resistance and estimating strength in resistance spot welding, Meas. Sci. Technol. 11 (2000) 1173–1178.
[22] P.X. Zhang, H.J. Zhang, J.H. Chen, Quality monitoring of resistance spot welding based on electrode displacement characteristics analysis, Front. Mech. Eng. China 2 (2007) 330–335.
[23] S.M. Hamidinejad, F. Kolahan, A.H. Kokabi, The modeling and process analysis of resistance spot welding on galvanized steel sheets used in car body manufacturing, J. Mater. Des. 34 (2012) 759–767.
[24] H.J. Zhang, Y.Y. Hou, Quality estimation of the resistance spot welding based on PCA–SVM, Hanjie Xuebao 30 (2009) 97–100.
[25] D.W. Zhao, Y.X. Wang, Z.G. Lin, S.N. Sheng., An effective quality assessment method for small scale resistance spot welding based on process parameters, NDT E Int. 55 (2013) 36–41.
[26] P. Podržaj, I. Polajnar, J. Diaci, Z. Kariž., Expulsion detection system for resistance spot welding based on a neural network, Meas. Sci. Technol. 15 (2004) 592–598.
[27] H.J. Zhang, Y.Y. Hou, X.W. Sui, Quality estimation of the resistance spot welding based on pattern feature of the electrode displacement signal, China Weld. 22 (2013) 53–58.
[28] O. Martín, M. López, F. Martin, Artificial neural networks for quality control by ultrasonic testing in resistance spot welding, J. Mater. Process. Technol. 183 (2006) 226–233.
[29] S.F. Ling, L.X. Wan, Y.R. Wong, D.N. Li, Input electrical impedance as quality monitoring signature for characterizing resistance spot welding, NDT E Int. 43 (2010) 200–205.
[30] H.J. Zhang, F.J. Wang, W.G. Gao, Y.Y. Hou, Quality assessment for resistance spot welding based on binary image of electrode displacement signal and probabilistic neural network, Sci. Technol. Weld. Join. 19 (2014) 242–249.
[31] M. Kimchi, Spot weld properties when welding with expulsion—a comparative study, Weld. J. 63 (1984) 58s–63s.
[32] M. Pouranvari, A. Abedi, P. Marashi, Effect of expulsion on peak load and energy absorption of low carbon steel resistance spot welds, Sci. Technol. Weld. Join. 18 (2008) 39–43.
[33] H. Chernoff., The use of faces to represent point in K-dimensional space graphically, J. Am. Stat. Assoc. 68 (1973) 361–368.
[34] R. Raciborski, Graphical representation of multivariate data using Chernoff faces, Stata J. 9 (2009) 374–387.
[35] Q.B. He, R.Q. Yan., F.R. Kong, R.X. Du, Machine condition monitoring using principal component representations, Mech. Syst. Signal Process. 23 (2009) 446–466.